Phys Chem Minerals (2002) 29: 291–299
DOI 10.1007/s00269-001-0233-3

ORIGINAL PAPER

N. Zotov · Y. Yanev · B. Piriou

Time-resolved luminescence of Fe^{3+} and Mn^{2+} ions in hydrous volcanic glasses

Received: 30 July 2001 / Accepted: 15 November 2001

Abstract Time-resolved luminescence spectra of natural and synthetic hydrous volcanic glasses with different colors and different Fe, Mn, and H_2O content were measured, and the implications for the glass structure are discussed. Three luminescence ranges are observed at about 380–460, 500–560, and 700–760 nm. The very short-living (lifetimes less than 40 ns) blue band (380–460 nm) is most probably due to the $^4T_2(^4D) \rightarrow {}^6A_1(^6S)$ and $^4A_1(^4G) \rightarrow {}^6A_1(^6S)$ ligand field transitions of Fe^{3+}. The green luminescence (500–560 nm) arises from the Mn^{2+} transition $^4T_1(^4G) \rightarrow {}^6A_1(^6S)$. It shows weak vibronic structure, short lifetimes less than 250 μs, and indicates that Mn^{2+} is tetrahedrally coordinated, occupying sites with similar distortions and ion–oxygen interactions in all samples studied. The red luminescence (700–760 nm) arising from the $^4T_1(^4G) \rightarrow {}^6A_1(^6S)$ transition of Fe^{3+} has much longer lifetimes of the order of several ms, and indicates that ferric iron is also mainly tetrahedrally coordinated. Increasing the total water content of the glasses leads to quenching of the red luminescence and decrease of the distortions of the Fe^{3+} polyhedra.

Present Address:
N. Zotov (✉)
Mineralogisch-Petrologisches Institut,
Universität Bonn,
53115 Bonn, Germany
Tel.: +49-228-732771; Fax: +49-228-732770
e-mail: nzotov@uni-bonn.de

N. Zotov
Bayerisches Geoinstitut,
Universität Bayreuth,
95540 Bayreuth, Germany

Y. Yanev
Geological Institute,
Bulgarian Academy of Sciences,
Sofia 1113, Bulgaria

B. Piriou
Laboratoire SPMS, Ecole Centrale de Paris,
92295 Chatenay-Malabry, France

Keywords Hydrous glasses · Fe^{3+} luminescence · Mn^{2+} luminescence

Introduction

Luminescence spectroscopy is a powerful method for studying trace elements and defects in minerals and glasses (Marfunin 1979; Waychunas 1988). Being an element-selective local probe of the structure, it can provide, similarly to extended X-ray fine structure absorption (EXAFS), X-ray absorption near-edge (XANES), and electron paramagnetic resonance (EPR) spectroscopies, information about the oxidation state and the coordination of the luminescence centers. In addition, due to the interaction of the electronic emission and absorption processes with lattice vibrations, it can provide information for their vibrational properties.

The luminescence of Fe^{3+} and Mn^{2+} centers in synthetic silicate, aluminosilicate, borosilicate, and phosphate glasses has been widely studied (Linwood and Weyl 1942; Bingham and Parke 1965; Kochibaya et al. 1969; Turner and Turner 1970; Parke 1971; Brawer and White 1978; Nelson and White 1980; Fox et al. 1981, 1982; Halilov and Pivovarov 1982; Menassa et al. 1986; Faber et al. 1987; Andrianasolo et al. 1989; Malashkevich et al. 1989; Nedelec et al. 1999). The main intervals of luminescence, observed in Fe^{3+}- and Mn^{2+}-containing silicate glasses and some crystalline phases doped with Fe^{3+} and Mn^{2+}, are summarized in Tables 1 and 2.

The luminescence of natural volcanic glasses, to the best of our knowledge, has not been investigated, mainly due to their usually high Fe^{3+} content (luminescence quenching) (Waychunas 1988). However, the color of volcanic glasses is mainly determined by the structural form of Fe and Mn present. On the other hand, the color of volcanic glasses is an important indicator for estimating the oxidation and the geological conditions during the cooling of acid magmas on the Earth's surface (Yanev 1988; Calas et al. 1988; Dormann et al. 1989; Yanev et al. 1993). Unfortunately, data on the

Table 1 Previous studies of Fe^{3+} luminescence in different silicate glasses and some Fe-doped crystalline phases

Glass composition (or mineral)	Position of the main luminescence peaks (nm)	Reference
Li–Si	714–720	Brawer and White (1978)
Na–Si	629, 690	Fox et al. (1982)
Si	455, 752	Malashkevich et al. (1989)
$LiAlO_2$	435, 455, 660–740 (77 K)	Palumbo (1971)
$LiAl_5O_8$	705 (77 K), 730	Melamed et al. (1972)
Adularia	711 (tetra)[a]	Telfer and Walker (1978)
Albite	716 (tetra)	Telfer and Walker (1978)
Orthoclase	690 (tetra)	White et al. (1986)
Forsterite	820–880 (tetra)	Walker and Glynn (1992)
Olivine	700 (tetra)	Bakhtin et al. (1995)
Willemite	746 (tetra) 1100 (octa)	Cavalli et al. (1995)
High-carnegieite	684 (tetra)	Nayak and Kutty (1998)

[a] The coordination of the Fe^{3+} dopand ion in the crystalline host is given *in parentheses*

Table 2 Previous studies of Mn^{2+} luminescence in different silicate glasses and some Mn-doped crystalline phases

Glass composition (or crystalline phase)	Position of the main luminescence peaks (nm)	Reference
Li–Na–Al–Si	570	Kochibaya et al. (1969)
K–Si	520, 640	Turner and Turner (1970)
Na–Mg–Ca–Al–Si	540, 630	Turner and Turner (1970)
Na–Si	520	Parke (1971)
Na–Si	535, 600	Nelson and White (1980)
Si	578	Halilov and Pivovarov (1982)
Li–Ca–Al–Si	540	Faber et al. (1987)
Na–B–Si	525, 550, 590	Menassa et al. (1986)
Li–Mg–Zn–Al–Si	535, 550	Andrianasolo et al. (1989)
Al_2O_3	600 (octa)[a]	McClure (1962)
Adularia	560 (tetra)	Telfer and Walker (1978)
Albite	560 (tetra)	Telfer and Walker (1978)
Calcite	630 (octa)	Marfunin (1979)
Forsterite	645 (octa)	Green and Walker (1985)
Olivine	630 (octa)	Bakhtin et al. (1995)
Spodumene	600 (octa)	Walker et al. (1997)
Willemite	522 (tetra)	Sohn et al. (1999)

[a] The coordination of the Mn^{2+} dopand ion in the crystalline host is given *in parentheses*

geometry of Fe^{3+} and Mn^{2+} sites in natural volcanic glasses are very scarce (Calas and Petiau 1983; Bershov et al. 1983; Henderson et al. 1995; Galoisy et al. 1999; Wu et al. 1999) and data on the effect of water on the luminescence of hydrous aluminosilicate glasses are practically non-existent, except for the paper of Zotov et al. (1992), which indicated that the Fe^{3+} luminescence peak at about 410–430 nm decreases with increasing water content.

Accordingly, in the present paper we present new luminescence data for different natural volcanic glasses with different Mn, Fe, and H_2O content and a different structural form of Fe^{3+} in order to investigate the coordination and site distortions of Fe^{3+} and Mn^{2+} as well as the effect of water on them.

Experimental

Sample description

Five synthetic and eight natural volcanic glasses are investigated. The synthetic glasses include (1) undoped sodium three-silicate glass $Na_2O{\cdot}3SiO_2$ (NS3), NS3 glass doped with 2 wt% Fe_2O_3, and NS3 glass doped with 2 wt% MnO. They were prepared using chemically pure SiO_2, Fe_2O_3 (MnO), and Na_2CO_3 melted at 1300 K in air atmosphere for 2 h and quenched in air; (2) three aluminosilicate glasses (denoted GW1, GW3, and GW5) with different water content (see Table 3), prepared from remelted Caucasus obsidian (Kecheldag deposit) in a hydrothermal bomb at 1300 K and 2 kbar pressure (for details see Zotov et al. 1992). The luminescence investigation of the latter gave the first indication of the feasibility of measuring luminescence spectra of Fe-containing natural hydrous glasses.

The natural samples include (1) white obsidian with less than 1 wt% water (archeological sample – obsidian knife from France); (2) several perlites from the periphery of volcanic domes from the Eastern Rhodopes, Bulgaria (age 37–30 Ma).

The chemical composition of the perlite samples was determined by wet, X-ray fluorescence, or microprobe analysis. The perlites have rhyolite composition (see Table 3) and are composed of volcanic glass and less than 10 vol% phenocrysts (quartz, sanidine, plagioclase, biotite, sometimes amphibole and/or clinopyroxene), accessories (magnetite, apatite, zircon), and feldspars and/or maphic microlites in different quantities. The different color depends mainly on the form of Fe^{2+} and Fe^{3+} present in the glass (Calas et al. 1988; Dorman et al. 1989; Yanev et al. 1993). The concentration of other trace elements in the samples which could also give luminescence was checked. Established are only Ce by NNA (with concentrations 40–120 ppm) and Cr by X-ray fluorescence (below 20 ppm).

Table 3 Chemical composition (wt%) of the studied natural and remelted (GW1, GW2, GW3) volcanic glasses

Sample	SiO_2	TiO_2	Al_2O_3	Fe_2O_3	FeO	MnO	MgO	CaO	Na_2O	K_2O	H_2O
GW1	77.0	0.04	12.90	0.63[g]	n.d.	n.d.	0.08	0.42	4.50	4.40	0.7
GW3	76.30	0.06	12.70	0.67[g]	n.d.	n.d.	0.15	0.43	3.70	3.80	3.0
GW5	73.50	0.05	12.20	0.62[g]	n.d.	n.d.	0.14	0.41	2.60	3.30	6.8
H–N[a]	66.68	0.30	15.15	2.34	0.72	0.07	0.50	1.66	3.97	5.64	2.63
HB–N[b]	74.01	0.08	12.26	n.d.	0.49[h]	0.05	0.04	0.45	2.67	5.99	4.12
HB–B[c]	74.16	0.08	12.26	n.d.	0.61[h]	0.07	0.03	0.49	2.84	5.74	3.72
SIL[d]	69.63	0.11	12.79	1.53	0.30	0.06	0.14	0.88	2.79	5.51	5.03
P–V[e]	72.69	0.10	11.69	0.96[g]	n.d.	417[i]	0.20	0.99	3.47	3.31	5.95
L–M[f]	70.02	n.d.	12.10	0.88[g]	n.d.	685[i]	0.22	0.85	3.09	3.78	6.04

[a] Black perlite from Hissar volcano, Bulgaria
[b] Black perlite from Haskovo mineral springs dome, Bulgaria
[c] White perlite from Haskovo mineral springs dome, Bulgaria
[d] White perlite from Silen vocano, Bulgaria
[e] Green perlite from the eastern part of the Borovitza caldera, Bulgaria
[f] Reddish-brown perlite from Lozen volcano, Bulgaria
[g] Total iron content calculated as Fe_2O_3
[h] Total iron content calculated as FeO
[i] In ppm

For comparison several crystalline phases were also measured: sanidine ($Or_{67.3}Ab_{32.1}An_{0.6}$) from one of the perlite samples (HB–B), olivine, transparent andradite (diamandite), hematite, and magnetite. No luminescence is detected for the last two minerals.

Luminescence measurements

The measurements were carried out on samples polished with diamond paste. For the perlite samples the excitation laser beam was focused on areas containing only volcanic glass. The experimental setup allows time-resolved spectroscopy to be performed and the luminescence decay profiles to be measured. The UV emission (337 nm) of a nitrogen laser (Jobin Yvon model LA01S) was used as excitation source. A lens ($f = 15$ cm) focused the beam on the sample. The spectral analysis of the luminescence was achieved by a Cary 14 monochromator equipped with a Hamamatsu photomultiplier (model R2658). A computer collected and processed the data. The time-resolved spectroscopy was performed by means of a digital oscilloscope (Tektronics, model 2430) coupled with the computer using home-made programs. Each luminescence decay following the excitation pulse was analyzed in real time during the scanning of the spectrum. Up to six times-resolved spectra can be recorded during one scan. The decay profiles were obtained by averaging over some hundred decay measurements. More details on this setup are given elsewhere (Piriou et al. 1994, 1996). Most of the measurements were carried out at 300 K and for two samples (GW1 and GW3) also at 77 K.

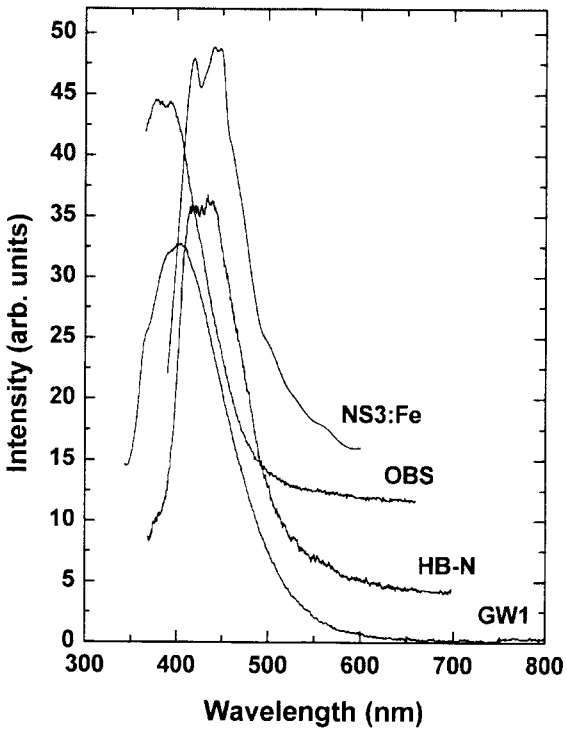

Fig. 1 Time-resolved blue emission spectra at room temperature: *GW1* delay 0.08 μs, gate 0.12 μs; *HB–N* delay 0.02 μs, gate 0.08 μs; *OBS*, obsidian knife, delay 0.02 μs, gate 0.08 μs; *NS3:Fe* delay 0.05 μs, gate 0.30 μs. The spectra are scaled to have the same intensity at the maximum and are shifted along the *y* axis for clarity

Results

In most of the investigated samples three ranges of luminescence are established: 380–460, 500–560, and 700-760 nm. These types of luminescence have different spectral characteristics, discussed below.

1. In the first, blue luminescence range a band with maxima at about 380–425, 440–445, and 460 nm is observed (see Fig. 1 and Table 4). The decay of this luminescence signal is very fast. For this reason it was measured with very short delay times of the order of ns (the theoretical time resolution of the scope is about 15 ns). The lifetimes are less than 40 ns and decrease with increasing water content (about 40 ns in GW1 at 77 K, about 25 ns in GW3 and less than 20 ns in GW5). Accordingly, in the perlite samples with high total water content (4 to 6 wt% H_2O) the signal is short-lived (< 20 ns) and difficult to measure.

2. The green luminescence in the range 500–560 nm is present in all samples except in the Mn-free NS3 sample (see Table 4 as well as Figs. 2 and 3). A strong band with a maximum at about 520–530 nm and two shoulders at about 500–515 nm and at about 540–560 nm is observed in the volcanic glasses. Contrary to the natural

glasses, the green band of the Mn^{2+}-doped NS3 sample is structureless, as is usually reported for Mn-doped synthetic glasses and crystalline phases. The full width at half maximum (FWHM) of the emission peak is practically the same in all samples studied. The decay of the luminescence signal (Fig. 4) cannot be explained by a single exponential function. The lifetimes are from 20 to 650 μs, much longer than those of the blue luminescence. The shortest lifetimes increase with increasing water content, while the longest lifetimes decrease with increasing water content. At 77 K the intensity of the green luminescence in GW1 and GW3 decreases dramatically compared to the red one.

3. The red luminescence in the range 700–760 nm is present in all investigated volcanic glasses and is absent in the iron-free NS3 sample. Only one very broad band with a maximum at about 700–750 nm is observed (in sanidine at 760 nm); see Figs. 2 and 3, except in the HB–B sample, where the spectrum after a long delay time (600 μs), shows some (vibronic) structure. The luminescence peak of the Fe-doped NS3 sample (peak maximum at about 720 nm) is similar to the spectrum published by Fox et al. (1982), although shifted to slightly higher wavelengths. For all samples, the red luminescence decay is nonexponential (see Fig. 5). From the tails of the decay curves we can estimate lifetimes from 1 to 2 ms. In all samples, the maximum of the red luminescence exhibits blue shift with increasing delay time (see Fig. 6). For this reason, in Table 4 the position of the red luminescence is given for the shortest delay time. At 77 K, on the contrary, a shift to higher wavelengths is observed with delay time (to 730 nm).

The red luminescence decays more slowly than the green luminescence (Fig. 5). Consequently, for a sample with a given total water content, the intensity of the green band decreases significantly with increasing delay time compared to the red band (Fig. 6). Similarly to the blue and the longest lifetimes of the green luminescence, the decay of the red luminescence becomes faster with increasing water content (see Fig. 7). Consequently, the intensity of the red band compared to the green one, for given time conditions, decreases with increasing total water content (see Fig. 3).

Discussion

The Fe^{3+} and Mn^{2+} ions are isoelectronic with $3d^5$ configuration. Their absorption and luminescence are well known. In accordance with the large literature on luminescence, as well as on the basis of our Fe- and Mn-doped NS3 glasses, the observed luminescence peaks may be interpreted as follows.

1. The short-lived peak in the range 380–460 nm has been scarcely studied and has been assigned to the emission from Fe^{3+} (Palumbo 1971; Melamed et al. 1972; Malashkevich et al. 1989). This is confirmed by the spectra of the Fe-doped NS3 sample in which it is very strong, with two peaks at about 415 and 440 nm. Most probably it is due to the $^4T_2(^4D) \rightarrow {}^6A_1(^6S)$ and $^4A_1(^4G) \rightarrow {}^6A_1(^6S)$ ligand field transitions. According to the Tanabe and Sugano (1954) diagram for ions with the $3d^5$ configuration, taking into account a Stokes shift of about 1700 cm^{-1}, as proposed by Fox et al. (1982), these two levels should be at about 430

Table 4 Luminescence maxima and decay times (τ) of the studied glasses and model compounds

Sample	Intervals of luminescence (nm)					
	380–460		500–560		700–760	
	max (nm)	τ (ns)	max (nm)	τ (μs)	max (nm)[a]	τ (ms)
SIL	–		510, 530, 550	60–235	730	
HB–B	–		510, 530, 560	35–240	730	2.0
HB–N	410, 440	< 20	500, 520, 550	55–250	730 vw[b]	
H–N	n.d.		505, 520, 550	40–235	750	
L–M	460	< 20	505, 520, 540	110–170	n.d.	
P–V	–		500, 520	90–250	720 vw[b]	
Obsidian knife	380, 395	~40	510, 530, 560	20–200	740	
GW1	400		515, 530, 550	20–650	720	< 0.004–1.8
GW1 (77 K)	415, 445, 460	~40	515, 530	n.d.	730	
GW3	420, 440, 460	~25	510, 530, 555	20–320	714	< 0.005–1.5
GW3 (77 K)	n.d.		515, 530	n.d.	730	
GW5	425, 460	~20	510, 530, 550	40–220	700	~1.8
NS3:Fe	415, 440	< 20	–		720	0.004–1.2
NS3:Mn	–		525	~600	–	
Olivine	430	< 20	–		–	
Andradite	440	< 20	–		–	
Sanidine	405	< 20	500, 520	45–200	760	

[a] The band positions are given for the shortest decay time because a blue shift occurs with increasing delay time
[b] vw – very weak

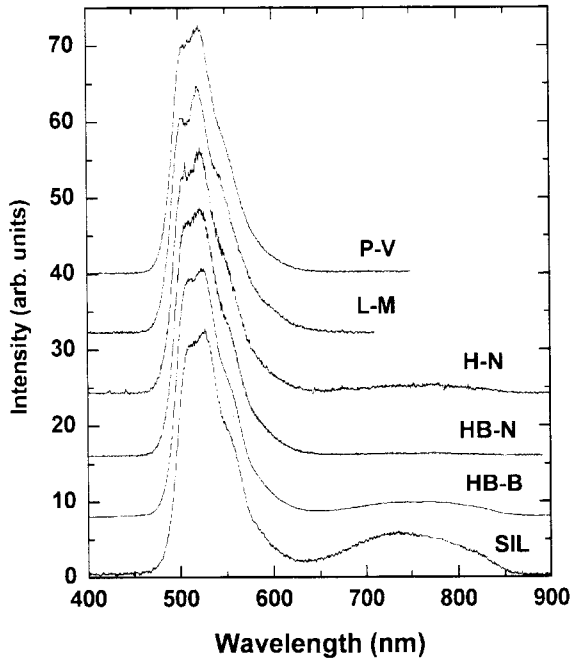

Fig. 2 Time-resolved green and red emission spectra at room temperature of natural volcanic glasses. Delay time 20 μs, gate 100 μs. The spectra are scaled to have the same intensity at 520 nm are shifted along the *y* axis for clarity

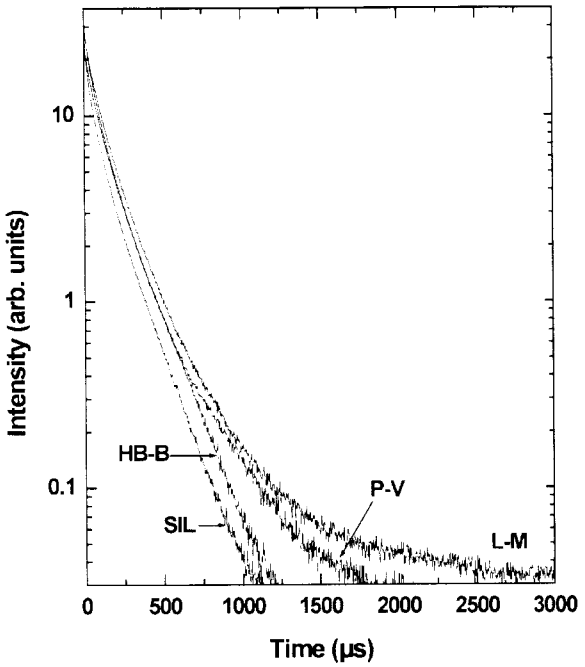

Fig. 4 Decay of the emission at 520 nm excited with 337 nm in different volcanic glasses at room temperature

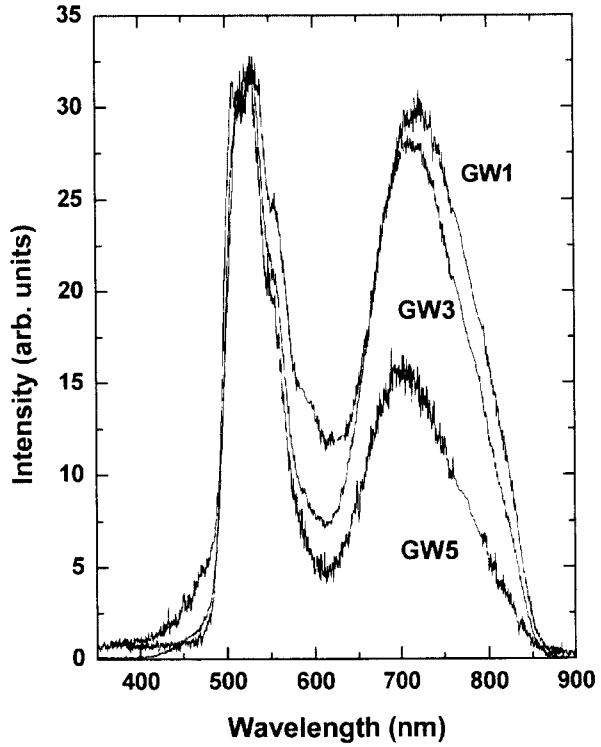

Fig. 3 Time-resolved emission spectra at room temperature of the remelted volcanic glasses. (*GW* samples). Delay time 20 μs, gate 100 μs. The spectra are scaled to have the same intensity at 520 nm

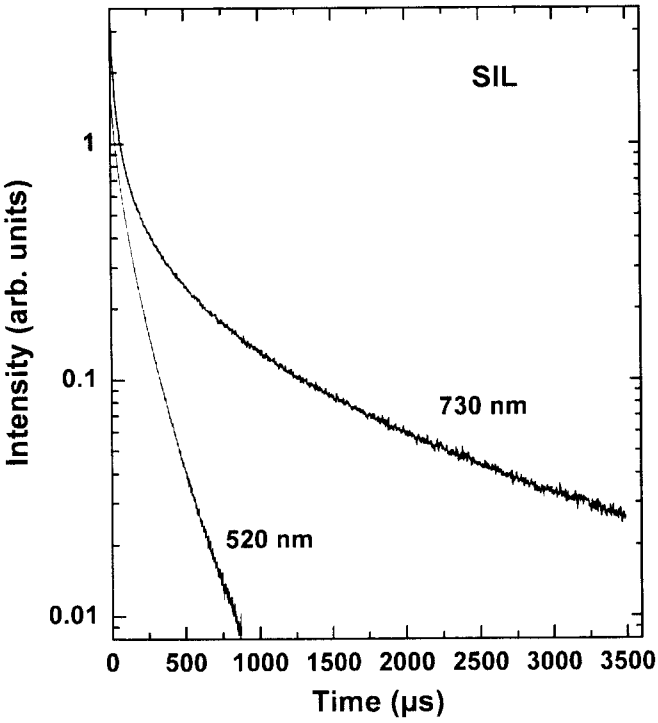

Fig. 5 Decay of the emissions at 520 and 730 nm excited with 337 nm in the *SIL* sample at room temperature

and 455 nm, respectively. The fast decay of this luminescence is probably due to vibrational deexcitation of the $^4T_2$ level towards the $^4T_1(^4G)$, the lowest emitting level. This luminescence peak in the investigated glasses is not due to $[AlO_4]^0$ defects (as suggested by Garcia-Guinea et al. 1998) because it is very strong in the Fe-doped NS3 glass, which is Al-free. However, we cannot rule out that it is partially due also to generic

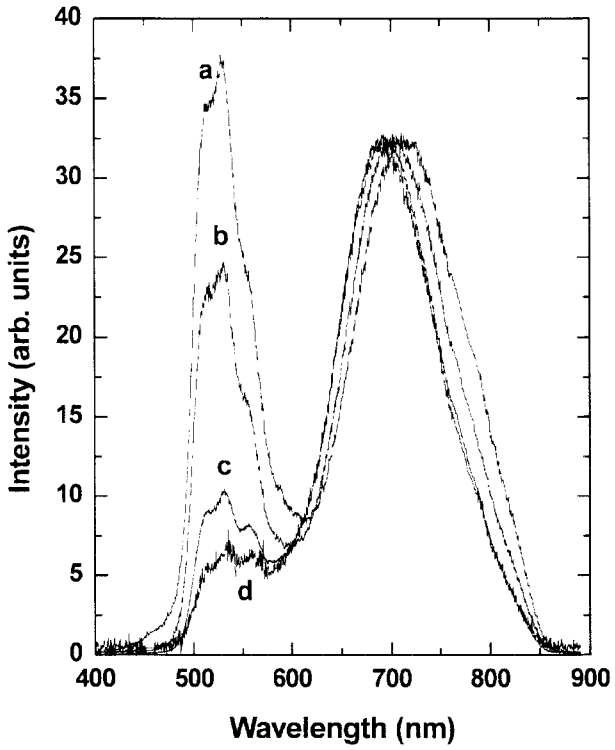

Fig. 6 Time-resolved luminescence spectra at room temperature of the GW3 sample with different delay and gate times: *a* delay 20 μs, gate 100 μs; *b* delay 120 μs, gate 300 μs; *c* delay 400 μs, gate 800 μs; *d* delay 600 μs, gate 800 μs. The spectra are scaled to have the same intensity at about 700 nm

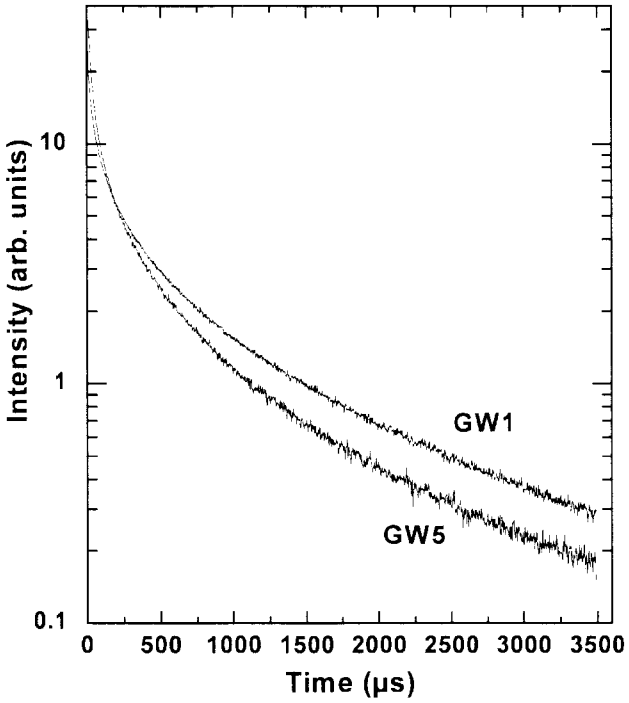

Fig. 7 Decay of the emission at 730 nm excited with 337 nm in the *GW1* and *GW5* sample

[SiO_4] defects, because weak blue emission is observed in silicates and even in high-purity silica polymorphs as well as in high-purity silica glass (Waychunas 1988; Bakhtin et al. 1995).

2. The green luminescence of about 500–555 nm is generally attributed to the transition $^4T_1(^4G) \rightarrow {}^6A_1(^6S)$ between the lowest energy levels of Mn^{2+} in tetrahedral coordination. Such a luminescence peak appears even at concentrations as low as 10 ppm (Adrianasolo et al. 1989). It cannot be excluded, however, that some Mn^{2+} ions occupy very large (dodecahedral) sites which can also produce small ligand field splitting Dq and green luminescence, respectively (McClure 1962; Noginov et al. 1999). The remarkable similarity of the position and the shape of the Mn^{2+} green emission band (Fig. 2), as well as the lack of luminescence peak at about 600–630 nm, typical for six-coordinated Mn^{2+} (see Table 2), strongly suggests that Mn^{2+} is tetrahedrally coordinated and occupies sites with similar ion–ligand interactions in all investigated volcanic glasses. At 77 K the position of the green luminescence peak in the GW1 and the GW3 samples remains practically the same (Table 4). The independence of the band position on temperature might indicate that Mn^{2+} occupies sites with rigid Mn–O bonds which practically do not change with temperature.

However, in comparison with binary Na_2O–SiO_2 glasses (Bingham and Parke 1965; Turner and Turner 1970; Parke 1971; Nelson and White 1980; Nedelec et al. 1999), the green luminescence in the investigated multicomponent hydrous volcanic glasses shows two shoulders at about 510–515 and 540–560 nm. Similar features were observed also in an Mn-doped multicomponent Li_2O–MgO–ZnO–Al_2O_3–SiO_2 glass (Andrianasolo et al. 1989). A vibronic origin of these features could be proposed. According to this assumption, the $^4T_1$ level should be coupled with some local vibrations of the MnO_4 species in the network. Alternatively, the two features could be due to raising the degeneracy of the energy levels involved in the $^4T_1 \rightarrow {}^6A_1$ transition due to local distortions of the tetrahedral symmetry. The luminescence spectra of GW3 taken at very long delay times ≥ 1600 μs (not shown in Fig. 6) indicate that the decay of the highest wavelength feature is longer than of the other two. This might indicate the presence of two kinds of Mn environments in the GW3 sample.

3. The red band at about 700–760 nm is attributed to the $^4T_1(^4G) \rightarrow {}^6A_1(^6S)$ transition of Fe^{3+}. On the time-resolved emission spectra of the Fe-doped NS3 sample measured with long delay times (greater than 50 μs) only this red band remains while the blue one vanishes. Since the same energy diagram applies to $3d^5$ cations in tetrahedral, octahedral, and cubic environments, the question of the ferric iron coordination should be specially discussed. The wavelength of the luminescent peak of four-coordinated Fe^{3+} in silicate glasses should be expected at about 690 nm (Fox et al. 1982) while for six-coordinated Fe^{3+}, observed mainly in phosphate glasses, it is at much lower energies – from 830 to 1200 nm (Fox et al. 1981). In Fe-doped orthoclase,

where Fe^{3+} is four-fold coordinated, the luminescent peak is at about 690 nm (Fox et al. 1982; White et al. 1986) or 711–716 nm (Telfer et al. 1978). The shift of the luminescence peak of octahedrally coordinated ferric iron to higher wavenumbers is consistent with the ligand field splitting in tetrahedral coordinated Dq(tet) being 4/9 of the ligand field splitting in octahedral coordination Dq(tet) = −4/9Dq(oct) (Burns 1993).

Therefore, the luminescence spectra indicate that the ferric iron in the investigated volcanic glasses is present mainly in tetrahedral coordination. Fe K-edge XANES studies of fully oxidized synthetic glasses with leucite-like composition, $MFe^{3+}Si_2O_6$ (M = K, Na), as well as natural pantellerite and Talasea obsidian glasses, clearly show that Fe^{3+} is dominantly four-coordinated (Henderson et al. 1995). Fe K-edge XANES spectra and ab initio full multiple-scattering simulations of submarine basalt glass also indicate that Fe^{3+} is mainly four fold-coordinated (Wu et al. 1993).

The red luminescent peak is shifted, however, to higher wavelengths compared to sanidine. This may indicate, first of all, larger distortions (larger Dq splittings) of the tetrahedral iron polyhedra in the glasses. Similar conclusions were drawn by Bershov et al. (1983) on the basis of EPR investigation of volcanic glasses. The red shift may indicate also presence of some five- and/or six-coordinated Fe^{3+}. For example, in tektite glasses a continuous distribution of four- and five-coordinated Fe^{3+} is established by Mössbauer spectroscopy (Rossano et al. 1999). It is also known (Vogel 1992) that during hydration of glasses the coordination of many three- and four-valent cations increases.

The decay of the red luminescence is much slower than that of the green luminescence (lifetimes of ms versus hundreds of μs). Typical decay curves of the green and the red luminescence from the SIL sample are shown in Fig. 5. Since the transitions of both Mn^{2+} and Fe^{3+} are spin-forbidden in tetrahedral symmetry, these results indicate that the Mn^{2+} site distortions lead to more efficient relaxation of the spin selection rule compared to Fe^{3+}. Alternatively, the difference in the lifetimes might indicate that the probability of radiationless transitions in the case of Fe^{3+} is much smaller.

The intensity of the red luminescence peak depends first of all on the amount of structural Fe^{3+} present in the glasses. Some of the investigated volcanic glasses with high iron content (samples H–N and L–M) exhibit very weak luminescence in this range because, according to their Mössbauer spectra (Dormann et al. 1989), the iron is present mainly in the form of mineral clusters with dimensions less than or equal to 15 nm as well as in the form of magnetite microlites with dimensions of a few microns. In these iron-rich clusters, a concentration quenching occurs similar to that in magnetite, where no emissions are observed. The structural iron in these glasses is below 0.1% of the total iron content in these samples. On the contrary, in the white volcanic glasses (like perlite SIL) the structural Fe^{3+} dominates (Yanev et al. 1993). Despite the fact that they have lower total Fe contents, they show much stronger red luminescence compared to the iron-rich perlites (see Fig. 2).

The red luminescence depends also on the total water content. The luminescence spectra of the model glasses GW1, GW3, and GW5 show that the relative intensity of the red luminescence decreases strongly with increasing total water content when compared to the green luminescence (Fig. 3). Examination of the GW samples under SEM showed that decrease of the red luminescence due to crystallization of magnetite can be ruled out. There are several possibilities for the interpretation of the observed decrease of the red luminescence with increasing total water content.

Fox et al. (1982) reported that the red luminescence at about 690 nm in Fe-doped binary sodium silicate glasses decreases on increasing the number of nonbridging oxygens (depolymerization of the glass structure). Although the mechanism of this luminescence quenching is still not completely understood, a similar mechanism could be envisaged for the natural hydrous rhyolite glasses as well. On the one hand, it is well established that water exists both as OH groups and molecular H_2O in these glasses (Bartholomew et al. 1980; Stolper 1982). On the other hand, X-ray diffraction and Raman spectroscopy (Zotov et al. 1992, 2000) indicate that water leads to depolymerization of the structure of rhyolite glasses via the formation of Si–OH bonds.

An alternative explanation could be the following. The presence of molecular H_2O may lead to the formation of some six-coordinated Fe^{3+} ions with H_2O molecules in the first coordination shell. This, in turn, would lead to a decrease of the luminescence because the transitions of Fe^{3+} in the octahedral crystal field are generally weaker in comparison with tetrahedral symmetry, since they are both spin- and parity-forbidden in octahedral symmetry (Imbusch 1978). The preferential location of H_2O to Fe^{3+} is in agreement with the stronger spectral dependence of the red luminescence band in comparison with the green band on the total water content.

We cannot of course, exclude some reduction of Fe^{3+} during the synthesis of the GW glasses in the hydrothermal bomb, but a similar decrease of the red luminescence is observed also for the natural hydrous volcanic glasses.

The red luminescence peak shifts also to smaller wavelengths with increasing total water contents. Since the $^4T_1(^4G)$ level has a negative slope as a function of the ligand field splitting Dq (at least for moderate Dq), the blue shift means that Dq decreases. In other words, the distortions of the Fe^{3+} coordination decrease with increasing water content. Taking into account that the crystal field splitting Dq is proportional to $1/R^5$ (Burns 1993), where R is the average cation-nearest neighbor distance, the decrease in Dq means that R increases with increasing total water content, which is plausible if Fe–OH bonds are formed. The decrease in the distortions of the Fe^{3+} tetrahedra would mean also that the lifetimes of the red luminescence should increase, which

where Fe^{3+} is four-fold coordinated, the luminescent peak is at about 690 nm (Fox et al. 1982; White et al. 1986) or 711–716 nm (Telfer et al. 1978). The shift of the luminescence peak of octahedrally coordinated ferric iron to higher wavenumbers is consistent with the ligand field splitting in tetrahedral coordinated Dq(tet) being 4/9 of the ligand field splitting in octahedral coordination Dq(tet) = −4/9Dq(oct) (Burns 1993).

Therefore, the luminescence spectra indicate that the ferric iron in the investigated volcanic glasses is present mainly in tetrahedral coordination. Fe K-edge XANES studies of fully oxidized synthetic glasses with leucite-like composition, $MFe^{3+}Si_2O_6$ (M = K, Na), as well as natural pantellerite and Talasea obsidian glasses, clearly show that Fe^{3+} is dominantly four-coordinated (Henderson et al. 1995). Fe K-edge XANES spectra and ab initio full multiple-scattering simulations of submarine basalt glass also indicate that Fe^{3+} is mainly four fold-coordinated (Wu et al. 1993).

The red luminescent peak is shifted, however, to higher wavelengths compared to sanidine. This may indicate, first of all, larger distortions (larger Dq splittings) of the tetrahedral iron polyhedra in the glasses. Similar conclusions were drawn by Bershov et al. (1983) on the basis of EPR investigation of volcanic glasses. The red shift may indicate also presence of some five- and/or six-coordinated Fe^{3+}. For example, in tektite glasses a continuous distribution of four- and five-coordinated Fe^{3+} is established by Mössbauer spectroscopy (Rossano et al. 1999). It is also known (Vogel 1992) that during hydration of glasses the coordination of many three- and four-valent cations increases.

The decay of the red luminescence is much slower than that of the green luminescence (lifetimes of ms versus hundreds of μs). Typical decay curves of the green and the red luminescence from the SIL sample are shown in Fig. 5. Since the transitions of both Mn^{2+} and Fe^{3+} are spin-forbidden in tetrahedral symmetry, these results indicate that the Mn^{2+} site distortions lead to more efficient relaxation of the spin selection rule compared to Fe^{3+}. Alternatively, the difference in the lifetimes might indicate that the probability of radiationless transitions in the case of Fe^{3+} is much smaller.

The intensity of the red luminescence peak depends first of all on the amount of structural Fe^{3+} present in the glasses. Some of the investigated volcanic glasses with high iron content (samples H–N and L–M) exhibit very weak luminescence in this range because, according to their Mössbauer spectra (Dormann et al. 1989), the iron is present mainly in the form of mineral clusters with dimensions less than or equal to 15 nm as well as in the form of magnetite microlites with dimensions of a few microns. In these iron-rich clusters, a concentration quenching occurs similar to that in magnetite, where no emissions are observed. The structural iron in these glasses is below 0.1% of the total iron content in these samples. On the contrary, in the white volcanic glasses (like perlite SIL) the structural Fe^{3+} dominates (Yanev et al. 1993). Despite the fact that they have lower total Fe contents, they show much stronger red luminescence compared to the iron-rich perlites (see Fig. 2).

The red luminescence depends also on the total water content. The luminescence spectra of the model glasses GW1, GW3, and GW5 show that the relative intensity of the red luminescence decreases strongly with increasing total water content when compared to the green luminescence (Fig. 3). Examination of the GW samples under SEM showed that decrease of the red luminescence due to crystallization of magnetite can be ruled out. There are several possibilities for the interpretation of the observed decrease of the red luminescence with increasing total water content.

Fox et al. (1982) reported that the red luminescence at about 690 nm in Fe-doped binary sodium silicate glasses decreases on increasing the number of nonbridging oxygens (depolymerization of the glass structure). Although the mechanism of this luminescence quenching is still not completely understood, a similar mechanism could be envisaged for the natural hydrous rhyolite glasses as well. On the one hand, it is well established that water exists both as OH groups and molecular H_2O in these glasses (Bartholomew et al. 1980; Stolper 1982). On the other hand, X-ray diffraction and Raman spectroscopy (Zotov et al. 1992, 2000) indicate that water leads to depolymerization of the structure of rhyolite glasses via the formation of Si–OH bonds.

An alternative explanation could be the following. The presence of molecular H_2O may lead to the formation of some six-coordinated Fe^{3+} ions with H_2O molecules in the first coordination shell. This, in turn, would lead to a decrease of the luminescence because the transitions of Fe^{3+} in the octahedral crystal field are generally weaker in comparison with tetrahedral symmetry, since they are both spin- and parity-forbidden in octahedral symmetry (Imbusch 1978). The preferential location of H_2O to Fe^{3+} is in agreement with the stronger spectral dependence of the red luminescence band in comparison with the green band on the total water content.

We cannot of course, exclude some reduction of Fe^{3+} during the synthesis of the GW glasses in the hydrothermal bomb, but a similar decrease of the red luminescence is observed also for the natural hydrous volcanic glasses.

The red luminescence peak shifts also to smaller wavelengths with increasing total water contents. Since the $^4T_1(^4G)$ level has a negative slope as a function of the ligand field splitting Dq (at least for moderate Dq), the blue shift means that Dq decreases. In other words, the distortions of the Fe^{3+} coordination decrease with increasing water content. Taking into account that the crystal field splitting Dq is proportional to $1/R^5$ (Burns 1993), where R is the average cation-nearest neighbor distance, the decrease in Dq means that R increases with increasing total water content, which is plausible if Fe–OH bonds are formed. The decrease in the distortions of the Fe^{3+} tetrahedra would mean also that the lifetimes of the red luminescence should increase, which

is observed at least for very short lifetimes in the GW samples (see Fig. 7).

Summary and conclusions

Time-resolved luminescence spectra of natural and synthetic hydrous aluminosilicate glasses have been measured. Three types of emission spectra are observed: blue, green, and red luminescence. The blue and the red luminescence are attributed to the presence of Fe^{3+}, the green luminescence to Mn^{2+} ions in the structure of the glasses. The decay of both the green and the red luminescence is nonexponential.

Analysis of the luminescence spectra shows that:

1. Mn^{2+} occupies a similar and well-defined tetrahedral site in all hydrous volcanic glasses studied. One possible scenario is that Mn^{2+} substitutes for Si^{4+} or Al^{3+} in the tetrahedral network, which might explain the rigidity of the Mn–O bonds. The Mn^{2+}–water interactions are weak and affect the lifetime of the green band only.

2. Fe^{3+} is mainly in tetrahedral coordination and occupies sites with larger distribution of static distortions, as indicated by the blue shift of the red band with increasing delay time.

3. The red luminescence from Fe^{3+} is very sensitive to the amount of structural iron in the glassy matrix.

4. The red luminescence from Fe^{3+} strongly decreases with increasing total water content. A possible mechanism for the luminescence quenching could be the depolymerization of the glass structure with increasing total water content and/or the formation of six-coordinated ferric iron ions with H_2O molecules as first nearest-neighbors. Additional XANES/EXAFS measurements would be necessary to check these results independently.

Acknowledgements One of the authors (Y. Yanev) would like to thank Prof. G. Calas of the University of Paris VI and VII for the financial support from MRT, France, during his stay in Paris.

References

Andrianasolo B, Champagnon B, Duvad E (1989) Behaviour of Mn^{2+} at very low concentrations in an aluminosilicate glass: luminescence properties and electron paramagnetic resonance. Phys Chem Glasses 30: 215–219

Bakhtin AI, Lopatin ON, Denisov IG (1995) Crystallochemical peculiarities of natural olivines by use of luminescent data. Geokhim 7: 967–973

Bartholomew RF, Butler BL, Hoover HL, Wu CK (1980) Infrared spectra of water-containing glass. J Am Cer Soc 63: 481–485

Bershov LV, Marfunin AS, Mineeva RM, Nasedkin VV (1983) Role of iron as stabilizer in the glass structure, (in Russian). Dokladi AN USSR, Ser Geol 11: 93–105

Bingham K, Parke S (1965) Absorption and fluorescence spectra of divalent manganese in glasses. Phys Chem Glasses 6: 224–232

Brawer SA, White WA (1978) Structure and crystallization behaviour of Li_2O–Fe_2O_3–SiO_2 glasses. J Mat Sci 13: 1907–1920

Burns R (1993) Mineralogical applications of crystal field theory. Cambridge University Press, Cambridge

Calas G, Petiau J (1983) Structure of oxide glasses: spectroscopic studies of local order and crystallochemistry. Bull Mineral 106: 33–35

Calas G, Angelov S, Yanev Y, Kostov R (1988) Electron paramagnetic resonance of perlites from Eastern Rhodopes, Bulgaria. Geol Balcan 18: 53–60

Cavalli E, Belletti A, Zannoni E (1995) Luminescence of Fe-doped willemite single crystals. J Sol State Chem 117: 16–20

Dormann JL, Djega-Mariadassou C, Yanev Y, Renaudin P (1989) Mössbauer study of mineral glasses: East Rhodopes perlites. Hyperfine Inter 46: 651–658

Faber AJ, Van Die A, Blasse G, Van der Weg WF (1987) Luminescence of manganese of different valencies in oxide glasses. Phys Chem Glasses 28: 150–155

Fox KE, Furukawa T, White WB (1981) Luminescence of Fe^{3+} in metaphosphate glasses: evidence for four- and six-coordinated sites. J Am Cer Soc 64: (C)42–(C)43

Fox KE, Furukawa T, White WB (1982) Transition metal ions in silicate melts, part 2. Iron in sodium silicate glasses. Phys Chem Glasses 23: 169–178

Galoisy L, Calas G, Arrio MA (2001) High-resolution XANES spectra of iron in minerals and glasses: structural information from the preedge region. Chem Geol 174: 307–319

Garcia-Guinea J, Rodriguez-Badiola E, Sanchez-Munoz L, Correcher V, Tookey A (1998) Luminescence spectra of leucite: some relations between thermal alkali loss and blue emission. Terra Nova Abstr Suppl 1, VII International Symposium on Experimental Mineralogy, Petrology and Geochemistry, 14–16 April, Orleans, France, p 19

Green GR, Walker G (1985) Luminescence excitation spectra of Mn^{2+} in synthetic forsterite. Phys Chem Miner 12: 271–278

Henderson CMB, Cressey G, Redfern SAT (1995) Geological applications of synchrotron radiation. Rad Phys Chem 45: 459–481

Halilov VH, Pivovarov SS (1982) Spectroscopic studies of the Mn^{2+} in silica glass, (in Russian). Fiz Khim Stekla 8: 311–317

Imbusch GF (1978) Inorganic luminescence. In: Lumb MD (ed) Luminescence spectroscopy. Academic Press, London

Kochibaya VI, Kikasheishvili TzV, Gavrilenko TB, Mikadze AZ (1969) Manganese-activated cathodoluminescent glasses, (in Georgian with Russian and English abstracts). Soobshtenia Acad Nauk Gruzinskoi SSR 54, 1: 53–56

Linwood SH, Weyl WA (1942) Fluorescence of manganese in glasses and crystals. J Opt Soc Am 32: 443–453

Malashkevich GE, Korjik ML, Livshitz MG, Pavlenko VB, Blinov AL, Borik MA (1989) Process of sensibilization and attenuation of luminescence of iron ions and lanthanides in silicate glasses, (in Russian). Fiz Khim Stekla 15: 675–687

Marfunin AS (1979) Spectroscopy, luminescence and radiation centers in minerals. Springer, Berlin Heidelberg New York, p 141

McClure DS (1962) Optical spectra of transition-metal ions in corrundum. J Chem Phys 36: 2757–2779

Melamed NT, Barros FS, Viccaro PJ, Artman JO (1972) Optical properties of Fe^{3+} in ordered and disordered $LiAl_5O_8$. Phys Rev (B) 5: 3377–3387

Menassa PE, Simkin DJ, Taylor P (1986) Spectroscopic investigations of Mn^{2+} in sodium borosilicate glasses. J Luminesc 35: 223–233

Nayak M, Kutty TRN (1998) Luminescence of Fe^{3+} doped $NaAlSiO_4$ prepared by gel to crystallite conversion. Mat Chem Phy 57: 138–146

Nedelec JM, Bouazaoui M, Turrell S (1999) Raman spectroscopic investigation of Mn^{2+} doping effects on the densification of acid-catalyzed silica xerogels. J Non-Cryst Solids 243: 209–219

Nelson C, White WB (1980) Transition metal ions in silicate melts – I. Manganese in sodium silicate melts. Geochim Cosmocim Acta 44: 887–893

Noginov MA, Loutts GB, Warren M (1999) Spectroscopic studies of Mn^{3+} and Mn^{2+} in $YAlO_3$. J Opt Soc Am (B) 16: 475–483

Palumbo DT (1971) Electronic states of Fe^{3+} in $LiAlO_2$ and $LiAl_5O_8$ phosphors. J Luminesc 4: 89–97

Parke S (1971) Effect of temperature on the fluorescence of divalent manganese in glasses. J Phys Chem Solids 32: 669–675
Piriou B, Dexpert-Ghys J, Mochizuki S (1994) Time-resolved photoluminescence spectra of MnO and MnS. J Phys Condens Matt 6: 7317–7327
Piriou B, Rager H, Schneider H (1996) Time-resolved fluorescence spectroscopy of Cr^{3+} in mullite. J Eur Cer Soc 16: 195–201
Rossano S, Balan E, Morin G, Bauer JP, Calas G, Brouder G (1999) Fe-57 Mössbauer spectroscopy of tektites. Phys Chem Miner 26: 530–538
Sohn KS, Cho B, Park HD (1999) Photoluminescence behaviour of manganese–doped zinc silicate phosphors. J Am Cer Soc 82: 2779–2784
Stolper EM (1982) Water in silicate glasses: an IR spectroscopic study. Contr Mineral Petrol 81: 1–17
Tanabe Y, Sugano S (1954) On the absorption spectra of complex ions, part II. J Phys Soc Jpn 9: 776–780
Telfer DJ, Walker G (1978) Ligand field bands of Mn^{2+} and Fe^{3+} luminescence centres and their site occupancy in plagioclase feldspars. Mod Geol 6: 199–210
Turner WH, Turner JE (1970) Absorption spectra and concentration-dependent luminescence of Mn^{2+} in silicate glasses. J Am Cer Soc 53: 329–334
Vogel W (1992) Glass chemistry. Springer, Berlin Heidelberg New York, p 466
Walker G, Glynn TJ (1992) Infra-red luminescence of iron-doped synthetic forsterite. J Luminesc 54: 131–137
Walker G, ElJaer A, Sherlock R, Glynn TJ, Czaja M, Mazurak Z (1997) Luminescence of Cr^{3+} and Mn^{2+} in spodumene ($LiAlSi_2O_6$). J Luminesc 72: 278–280
Waychunas GA (1988) Luminescence, X-ray emission and new spectroscopies. In: Howthorne FC (ed) Spectroscopic methods in mineralogy and geology. Reviews in Mineralogy, vol 18. Mineralogical Society of America, Washington DC, pp 639–698
White WB, Matsumura M, Linnehan DG, Furukawa T, Chandrasekhar BK (1986) Absorption and luminescence of Fe^{3+} in single-crystal orthoclase. Am Mineral 71: 1415–1419
Wu Z, Bonnin-Mosbah M, Duraud JP, Metrich N, Delaney JS (1999) XANES studies of Fe-bearing glasses. J Synchrot Rad 6: 344–346
Yanev Y (1988) Characterization of volcanic glasses from Eastern Rhodopes, Bulgaria. In: Konta J (ed) IInd International Conference on Natural Glasses, University Karlova, Prague, pp 129–138
Yanev Y, Calas G, Dormann JL (1993) Form of Fe in the Eastern Rhodopes perlites (Bulgaria): EPR and Mössbauer studies. Terra Nova Abstr Suppl 1, EUG VII, p 565
Zotov N, Yanev Y, Epelbaum M, Konstantinov L (1992) Effect of water on the structure of rhyolite glasses – X-ray diffraction and Raman spectroscopy studies. J Non-Cryst Solids 142: 234–246
Zotov N, Sowerby J, Keppler H (2000) Structure of hydrous rhyolite and basalt glasses: Raman spectroscopic study. VIII International Symposium on Experimental Mineralogy, Petrology and Geochemistry (EMPG VIII), 16–19 April, Bergamo, Italy